ACS OMEGA

http://pubs.acs.org/journal/acsodf

Article

Crystal Growth, Single Crystal Structure, and Biological Activity of Thiazolo-Pyridine Dicarboxylic Acid Derivatives

Hamdi Ben Yahia,* Souhir Sabri, Rachid Essehli, Peter Kasak, Joanna Drogosz-Stachowicz, Anna Janecka, and Brahim El Bali

Cite This: *ACS Omega* 2020, 5, 27756−27765

Read Online

ACCESS | Metrics & More | Article Recommendations | Supporting Information

ABSTRACT: Four novel TPDCA derivatives were prepared via a supersaturation method combining TPDCA with water, *N*-methyl-2-pyrrolidone (NMP), $Na(PO_2H_2)$, and ammonia solution: $2(C_9H_7NO_5S)\cdot H_2O$ (**1**), $(C_9H_7NO_5S)C_5H_9NO$ (**2**), $(C_9H_7NO_5S)Na(PO_2H_2)$ (**3**), and $(C_9H_5NO_5S)(NH_4)_2(H_2O)$ (**4**). Their crystal structures were determined by single-crystal X-ray diffraction. Compounds (**1**) and (**2**) crystallize in the monoclinic space groups $P2_1$ and $P2_1/c$, respectively, whereas compounds (**3**) and (**4**) crystallize in the triclinic space group $P\bar{1}$. Weak and moderate hydrogen bonds were detected in the four compounds. In the biological tests, (**1**) and (**3**) exhibited significant antibacterial activity against *Escherichia coli* and *Staphylococcus aureus*; in addition, (**1**) was cytotoxic against leukemia HL-60 cells with the IC_{50} value of 158.5 ± 12.5 μM.

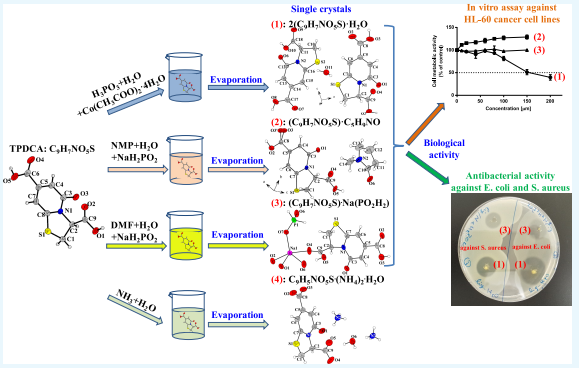

1. INTRODUCTION

Ring-fused 2-pyridone structural fragment can be found in many natural products and biologically active compounds, and its derivatives have shown potential as anticancer drugs,[1] antibacterial agents,[2] or protein−protein interaction inhibitors.[3] Recently, ring-fused 2-pyridones started to attract much attention as easily accessible molecular fluorophores for application in luminescent materials.[4,5] Such fluorescent compounds can be easily prepared by condensation of citric acid with α-heteroatom-containing β-amines.[6,7] For example, multistep condensation of citric acid and L-cysteine leads to formation of the fluorescent derivative 5-oxo-2,3-dihydro-5H-[1,3]-thiazolo[3,2-a]pyridine-3,7-dicarboxylic acid (TPDCA / $C_9H_7N_1O_5S$), which was identified as a main source of molecular fluorescence in luminescent gels,[8] biodegradable polymers,[9,10] and carbon dots[11] or applied in a low-cost material for chloride sensing in the diagnosis of cystic fibrosis.[12] Bicyclic 2-pyridone derivatives, termed pilicides, are compounds that inhibit the formation of virulence-associated organelles termed pili.[13] Pilicides are also considered a promising alternative or complementary therapeutics to the monoclonal antibodies in cancer therapy.[14] In the study published by Horvath et al. the authors demonstrated that ring-fused 2-pyridones triggered fibrillization of a key protein in Parkinson's disease, α-synuclein.[15] In a recent paper by Kulén et al., the methyl sulfonamide substituents were shown to enhance the pharmacokinetic properties of bicyclic 2-pyridone-based Chlamydia trachomatis inhibitors.[16]

In this study, using a single crystal X-ray diffraction method, we investigated the crystal structures of four novel derivatives with general formulas $2(C_9H_7NO_5S)\cdot H_2O$, $(C_9H_7NO_5S)$-C_5H_9NO, $(C_9H_7NO_5S)Na(PO_2H_2)$, and $(C_9H_5NO_5S)$-$(NH_4)_2(H_2O)$ prepared by combining TPDCA with water, *N*-methyl-2-pyrrolidone (NMP), $Na(PO_2H_2)$, and ammonia solution, respectively. Antibacterial and cytotoxic properties of the novel compounds were also evaluated.

2. RESULTS AND DISCUSSION

2.1. Structure Refinement. *2.1.1. Structure Refinement of Compound (1).* The systematic absences 0k0: k = 2n indicated the possible space groups $P2_1$ and $P2_1/m$. The structure was determined using the non-centrosymmetric space group $P2_1$, and the latter was confirmed using the Platon suite of programs, which did not suggest the existence of any higher symmetry.[17−19] All the O, N, S, and C atomic positions were located using the superflip program implemented in the Jana2006 program package. With isotropic ADPs, the residual factors converged to the value $R(F)$ = 0.1362 and $wR(F^2)$ = 0.2104 (*G.O.F.* = 3.13) for 133 refined parameters and 4213 observed reflections. At this stage of the refinement, the

Received: April 17, 2020
Accepted: July 6, 2020
Published: October 22, 2020

Table 1. Experimental Details[a]

parameter	(1)	(2)	(3)	(4)
crystal data				
chemical formula	$2(C_9H_7NO_5S)\cdot H_2O$	$(C_9H_7NO_5S)\cdot C_5H_9NO$	$(C_9H_7NO_5S)\ Na(PO_2H_2)$	$C_9H_5NO_5S\ (NH_4)_2\ H_2O\cdot$
M_r	500.4	340.4	329.2	293.3
crystal system, space group	monoclinic, $P2_1$	monoclinic, $P2_1/c$	triclinic, $P\bar{1}$	triclinic, $P\bar{1}$
temperature (K)	293	293	150	293
a, b, c (Å)	6.2294 (8), 9.8153 (16), 17.133 (3)	14.7840 (9), 6.8291 (4), 16.0750 (8)	6.2307 (3), 9.0432 (4), 11.7429 (5)	5.6564 (3), 10.7717 (6), 11.2333 (6)
α, β, γ (°)	90, 92.880 (5), 90	90, 106.460 (2), 90	97.642 (2), 93.975 (2), 103.694 (2)	67.751 (2), 80.440 (2), 83.967 (2)
V (Å^3)	1046.2 (3)	1556.44 (15)	633.64 (5)	624.01 (6)
Z	2	4	2	2
radiation type	Mo $K\alpha$	Mo $K\alpha$	Mo $K\alpha$	Mo $K\alpha$
μ (mm^{-1})	0.32	0.24	0.45	0.29
crystal size (mm)	0.18 × 0.07 × 0.02	0.24 × 0.09 × 0.08	0.16 × 0.1 × 0.08	0.22 × 0.08 × 0.05
data collection				
diffractometer	D8 Venture diffractometer	D8 venture diffractometer	D8 venture diffractometer	D8 Venture diffractometer
absorption correction	Gaussian processed with Jana2006	Gaussian processed with Jana2006	multiscan processed with *SADABS*	multiscan processed with *SADABS*
T_{min}, T_{max}	0.96, 0.99	0.967, 0.985	0.704, 0.749	0.92, 0.98
no. of measured, and independent reflections	21,038, 4325	21,605, 3314	8781, 3842	9883, 3089,
no. of observed reflections	4212 [$I > 0\sigma(I)$]	2606 [$I > 2\sigma(I)$]	3689 [$I > 0\sigma(I)$]	2144 [$I > 3\sigma(I)$]
R_{int}	0.045	0.057	0.02	0.033
$(\sin\theta/\lambda)_{max}$ (Å^{-1})	0.628	0.635	0.715	0.667
refinement				
$R[F^2 > 2\sigma(F^2)]$, $wR(F^2)$, S	0.039, 0.077, 1.09	0.042, 0.132, 1.14	0.043, 0.108, 1.19	0.035, 0.112, 1.12
no. of reflections	4325	3314	3842	3089
no. of parameters	318	218	196	185
no. of restraints	7	2	2	5
$\Delta\rho_{max}$, $\Delta\rho_{min}$ (e Å^{-3})	0.13, −0.12	0.19, −0.16	0.37, −0.23	0.30, −0.19

[a]The H atoms were treated by a mixture of independent and constrained refinement.

chemical formula is $2(C_9H_0NO_5S)H_0O$. With anisotropic ADPs, the residual factors converged to the value $R(F)$ = 0.0663 and $wR(F^2)$ = 0.1497 (*G.O.F.* = 1.54) for 298 refined parameters. The CH hydrogen atoms were placed in calculated positions with $U_{iso}(H)$ = 1.2 $U_{eq}(C)$, whereas the OH hydrogen atoms were determined from the Fourier difference maps with $U_{iso}(H)$ = 1.2 $U_{eq}(O)$. The C−H and COO−H distances were constrained/restrained to 0.96 Å. Two restrains were applied to the water molecule. The O−H distances and the H−O−H angle were set to 0.960 Å and 104.45°, respectively. This led to the final chemical formula $2\text{-}(C_9H_7NO_5S)H_2O$. By refining the Flack[20] and the extinction parameters, the residual factors converged to the values given in Table 1. The refined atomic positions and anisotropic ADPs are given in Tables S1 and S2, respectively. The collected data for compound (**1**) is from a twin crystal with a twin fraction of 0.38 (5).

*2.1.2. Structure Refinement of Compound (**2**).* The systematic absences h0l: l = 2n and 0k0: k = 2n indicated that the space group is $P2_1/c$. All the O, N, S, and C atomic positions were located using the superflip program. With anisotropic ADPs, the residual factors converged to the value $R(F)$ = 0.0662 and $wR(F^2)$ = 0.1881 (*G.O.F.* = 1.85) for 209 refined parameters and 2606 observed reflections. At this stage of the refinement, the chemical formula is $(C_9H_0NO_5S)\text{-}C_5H_0NO$ with large ADPs for O3. Therefore, the atomic position of O3 was split. The CH hydrogen atoms were placed in calculated positions with $U_{iso}(H)$ = 1.2 $U_{eq}(C)$, whereas the OH hydrogen atoms were determined from the Fourier difference maps with $U_{iso}(H)$ = 1.2 $U_{eq}(O)$. The C−H and COO−H distances were constrained/restrained to 0.96 Å. This led to the final chemical formula $(C_9H_7NO_5S)C_5H_9NO$. By refining the extinction parameter, the residual factors converged to the values given in Table 1. The refined atomic positions and anisotropic ADPs are given in Tables S3 and S4, respectively.

*2.1.3. Structure Refinement of Compound (**3**).* The structure was determined using the space group $P\bar{1}$. The heaviest atoms were located using the superflip program. With isotropic ADPs, the residual factors converged to the value $R(F)$ = 0.1693 and $wR(F^2)$ = 0.2754 (*G.O.F.* = 3.06) for 82 refined parameters and 3689 observed reflections. At this stage of the refinement, the chemical formula is $(C_9H_0NO_5S)\text{Na-}(PO_2H_0)$. With anisotropic ADPs, the residual factors converged to the value $R(F)$ = 0.063 and $wR(F^2)$ = 0.1807 (*G.O.F.* = 2.04) for 182 refined parameters. The CH hydrogen atoms were placed in calculated positions with $U_{iso}(H)$ = 1.2 $U_{eq}(C)$, whereas the OH hydrogen atoms were determined from the Fourier difference maps with $U_{iso}(H)$ = 1.2 $U_{eq}(O)$. The C−H and COO−H distances were constrained/restrained to 0.96 Å. This led to the final chemical formula $(C_9H_7NO_5S)\text{-}Na(PO_2H_2)$. By refining the extinction parameter, the residual factors converged to the values given in Table 1. The refined atomic positions and anisotropic ADPs are given in Tables S5 and S6, respectively.

*2.1.4. Structure Refinement of Compound (**4**).* The structure was determined using the space group $P\bar{1}$. The C, O, N, and S atoms were located using the superflip program.

https://dx.doi.org/10.1021/acsomega.0c01769
ACS Omega 2020, 5, 27756−27765

With isotropic ADPs, the residual factors converged to the value $R(F)$ = 0.1149 and $wR(F^2)$ = 0.2934 (*G.O.F.* = 3.48) for 77 refined parameters and 3089 observed reflections. At this stage of the refinement, the chemical formula is $(C_9H_0NO_5S)(NH_0)_2(H_0O)$. With anisotropic ADPs, the residual factors converged to the value $R(F)$ = 0.067 and $wR(F^2)$ = 0.1983 (*G.O.F.* = 2.41) for 172 refined parameters. The CH hydrogen atoms were placed in calculated positions with $U_{iso}(H)$ = 1.2 $U_{eq}(C)$, whereas the OH and NH hydrogen atoms were determined from the Fourier difference maps with $U_{iso}(H)$ = 1.2 U_{eq}(O or N). The C−H, COO−H and N−H distances were set to 0.96, 0.96 ± σ and 0.87 ± σ Å, respectively. Two restrains were applied to the water molecule. The O−H distances and the H−O−H angle were set to 0.960 Å and 104.45°, respectively. This led to the final chemical formula $(C_9H_5NO_5S)(NH_4)_2(H_2O)$. By refining the extinction parameter, the residual factors converged to the values given in Table 1. The refined atomic positions and anisotropic ADPs are given in Tables S7 and S8, respectively. Further details on the structure refinements of (**1**), (**2**), (**3**), and (**4**) may be obtained from the Cambridge Crystallographic Data Centre (CCDC), by quoting the registry no. CCDC-1985955, no. CCDC-1985956, no. CCDC-1985957, and no. CCDC-1985958, respectively.

2.2. Crystal Structure. *2.2.1. Crystal Structure of Compound (1).* Compound (**1**) crystallizes in the monoclinic space group $P2_1$. The asymmetric unit consists of one water molecule and two symmetry-independent TPDCA molecules. The latter are denoted L1 for S1N1C1-C9 and L2 for S2N2C10-C18 (Figure 1).[21] A packing diagram of (**1**), viewed down the *a* axis, is given in Figure 2a. In L1, the five-membered rings have a substantially flattened envelope conformation with a dihedral angle of 21.38° between the C2C1S1 fragment and the C2N1C7S1 plane (Figure 1). The puckering parameters *Q* = 0.226 (2) Å and φ = 43.2 (5)° and the pseudorotation parameters *P* = 212.6 (3)° and Tau(*M*) = 22.2 (1)° for the reference bond S1-C1 suggest an envelope conformation on C1. The interatomic S1-C1 and S1-C7 distances of 1.810 (3) Å and 1.734 (2) Å are typical of the S-Csp^3 and S-Csp^2 bonds, respectively.[11,22,23] The bicyclic S1N1C2-C8 system can be regarded as planar since the dihedral angle between the six- and five-membered rings is only 4.01°. The carboxyl group C8O2O3H is almost co-planar with the bicyclic fragment with a dihedral angle of 6.01°. The carboxyl group C9O4O5H is almost perpendicular to the bicyclic fragment with a dihedral angle of 74.58°.

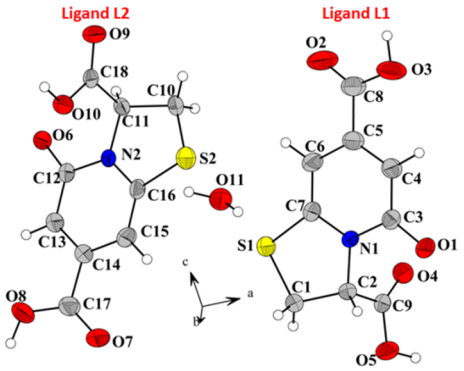

Figure 1. View of the molecular structure of (**1**), showing 50% probability displacement ellipsoids. H atoms are shown as small spheres of arbitrary radii.

Comparing to L1, in L2, the five-membered rings have a less-flattened envelope conformation with a dihedral angle of 31.59° between the C11C10S2 fragment and the C11N2C16S2 plane (Figure 1). The puckering parameters *Q* = 0.3323 (18) Å and φ = 216.9 (3)° and the pseudorotation parameters *P* = 25.7 (2)° and Tau(*M*) = 31.6 (1)° for the reference bond S2-C10 suggest an envelope conformation on C10. The bicyclic S2N2C11-C17 fragment can be regarded as approximately planar since the dihedral angle between the six- and five-membered rings is 6.02°. The carboxyl group C17O7O8H is rotated by 21.54° from its attached ring. The carboxyl group C18O9O10H is almost perpendicular to the thiazolopyridine group with a dihedral angle of 80.68°. This is very similar to the dihedral angle of 83° observed in the unsolvated TPDCA structure.[11] The crystal structure of (**1**) is stabilized by moderate and weak hydrogen bonds.[24,25] Selected bond lengths and angles are given in Table 2. For clarity reasons, different colors have been used to distinguish between the different types of hydrogen bonds. The blue lines correspond to the O−H···O hydrogen bonds involving water molecules and carboxyl H and O atoms and amide keto O atoms of neighboring molecules (Figure 2c). The red and green lines correspond to the O−H···O and C−H···O hydrogen bonds, respectively, that do not involve water molecules (Figure 2d). These hydrogen bonds link the different molecules to form a 3D framework. Furthermore, symmetry equivalent L2 ligands interact via C═O···π (orange) interactions [O9-*Cg*5i = 3.5427 (18) Å, C18-O9-*Cg*5 angle = 146.35 (12)°, *Cg*5 is the centroid of the six-membered ring (N2C12-C16), symmetry code (i): $-x,-1/2 + y,1 - z$] (Figure 2b). The additional $\pi-\pi$ stacking interactions between L1 and L2 ligands are too weak to be taken in consideration [*Cg*2-*Cg*5ii = 5.1111 (15) Å, interplanar distance = 3.3750 (8) Å, slippage = 4.0738 (8) Å, α = 10.4812 (7)°, β = 17.45 (10)°, γ = 37.15 (2)°, *Cg*2 and *Cg*5 are the centroids of the six-membered rings in the ligands L1 and L2, respectively, symmetry code (ii): $1 + x,y,z$] (Figure 2b).

2.2.2. Crystal Structure of Compound (2). Compound (**2**) crystallizes in the monoclinic space group $P2_1/c$ with one NMP and one TPDCA molecules in the asymmetric unit (Figure 3). A packing diagram of (**2**), viewed down the *b* axis is given in Figure 4. One can clearly distinguish layers of TPDCA molecules in the (100) plane separated by a NMP layer. The NMP molecules are perfectly flat with slightly high ADPs of all atoms. They are almost perpendicular to the bicyclic fragment with a dihedral angle of 86.35°.

The structure of (**2**) contains bent hydrogen bonds.[24] All these bonds are moderate based on the classification of Jeffrey.[25] Selected bond lengths and angles are given in Table 3. Each TPDCA molecule is interconnected to two other TPDCA molecules and one NMP molecule through COO−H···O═C hydrogen bonds, forming one-dimensional infinite chains along the [001] direction (see blue and green dashed line in Figure 4 and Figure S1). Furthermore, the NMP molecules of neighboring chains interact through C═O···π interactions [C10-O6···*Cg*2ii = 3.665 (2) Å, *Cg*4ii is the centroid of the NMP ring (N2C10-C13), symmetry code (ii): $1 - x,-1/2 + y,1/2 - z$] (see brown dashed line in Figure 4). The offset $\pi-\pi$ interactions between TPDCA molecules [*Cg*3-*Cg*3i = 4.192 (1) Å, interplanar distance = 3.502 (1) Å, slippage = 2.304 (1) Å, α = 0.03 (7)°, *Cg*3 is the centroid of

https://dx.doi.org/10.1021/acsomega.0c01769
ACS Omega 2020, 5, 27756−27765

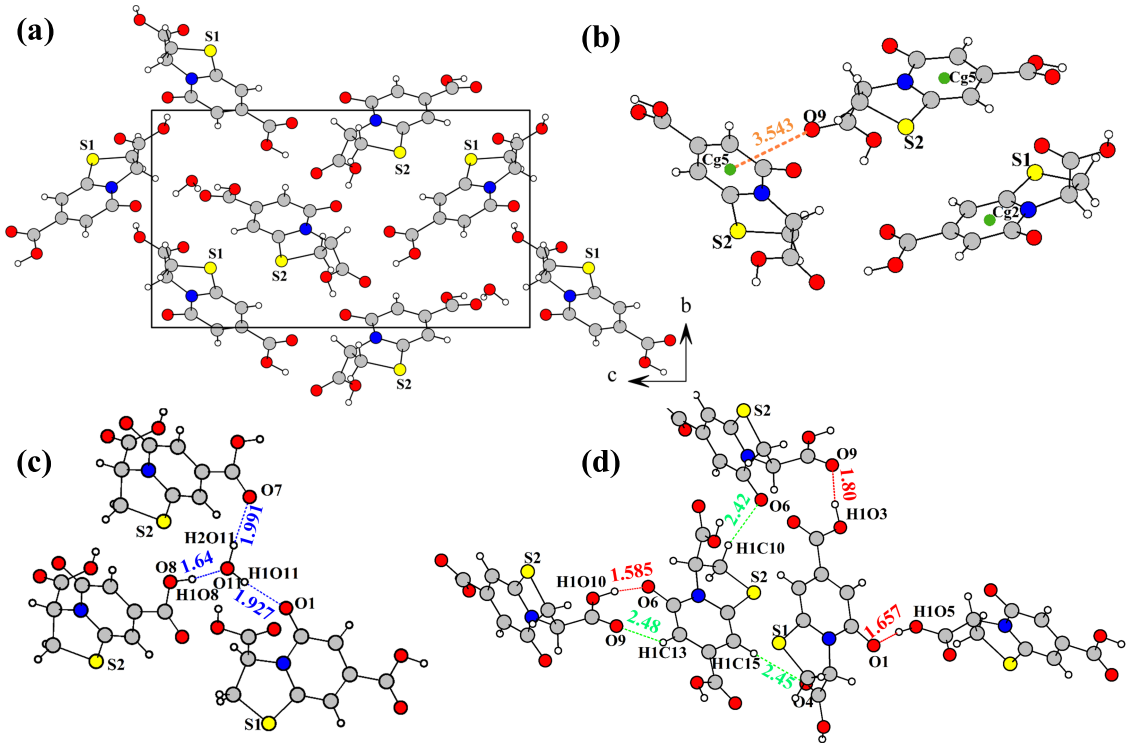

Figure 2. (a) Packing diagram of (**1**) viewed down the *a* axis. (b) C═O···π (orange) interactions. *Cg*2 and *Cg*5 are the centroids of the six-membered rings in the ligands L1 and L2, respectively. (c) Hydrogen bonds involving the water molecule (blue dashed lines). (d) Hydrogen bonds, which do not involve water molecules. The red and green dashed lines correspond to the O−H···O and C−H···O hydrogen bonds, respectively.

Table 2. List of Detected Hydrogen Bonds in (1)

donor	hydrogen	acceptor	D−H distance	H···A distance	D−A distance	D−H···A angle
C10	H1C10	O6	0.96	2.42	3.350(3)	163.58
C13	H1C13	O9	0.96	2.48	3.316(3)	144.84
C15	H1C15	O4	0.96	2.45	3.391(3)	168.29
O3	H1O3	O9	0.96(2)	1.80(2)	2.716(3)	160(3)
O5	H1O5	O1	0.960(18)	1.657(17)	2.610(2)	172(2)
O10	H1O10	O6	0.960(17)	1.585(19)	2.521(2)	163.8(17)
O8	H1O8	O11	0.960(19)	1.64(2)	2.592(2)	169(2)
O11	H1O11	O1	0.960(19)	1.927(18)	2.834(2)	156.6(17)
O11	H2O11	O7	0.960(16)	1.991(14)	2.933(3)	166.6(18)

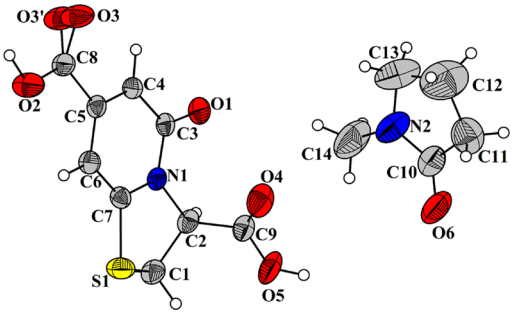

Figure 3. View of the molecular structure of (**2**), showing 50% probability displacement ellipsoids. H atoms are shown as small spheres of arbitrary radii.

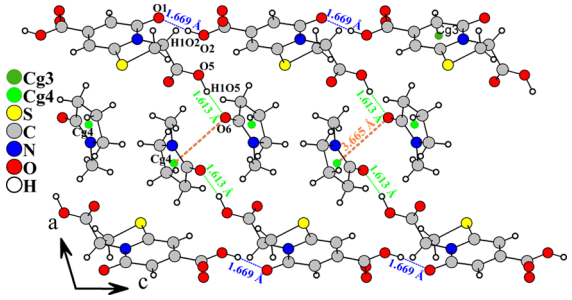

Figure 4. View of the structure of (**2**) down the *b* axis showing intermolecular interactions. The O−H···O blue dashed lines interconnect TPDCA molecules, whereas the green dashed lines interconnect TPDCA to NMP molecules. The brown lines correspond to C═O···π interactions within the NMP layer.

the six-membered ring (N1C3-C7), symmetry code (i): 2 − *x*,1 − *y*,−*z*] and between the NMP molecules [*Cg*4-*Cg*4i = 5.546 (2) Å, interplanar distance = 3.875 (1) Å, slippage = 3.958 (1) Å, α = 0.03 (7)°, *Cg*4 is the centroid of the NMP ring (N2C10-C13), symmetry code (i): 1 − *x*,2 − *y*,−*z*] were not taken into consideration since they are too weak (see the yellow and pink dashed lines in Figure S1).

https://dx.doi.org/10.1021/acsomega.0c01769
ACS Omega 2020, 5, 27756−27765

Table 3. List of Detected Hydrogen Bonds in (2)

donor	hydrogen	acceptor	D−H distance	H···A distance	D−A distance	D−H···A angle
O2	H1O2	O1	0.96(2)	1.67(2)	2.603(2)	164(2)
O5	H1O5	O6	0.956(18)	1.614(19)	2.555(3)	167(2)

2.2.3. Crystal Structure of Compound (3). Compound (**3**) crystallizes in the triclinic space group *P*-1 with one TPDCA and one sodium hypophosphite salt molecules in the asymmetric unit (Figure 5). The structure is layered parallel

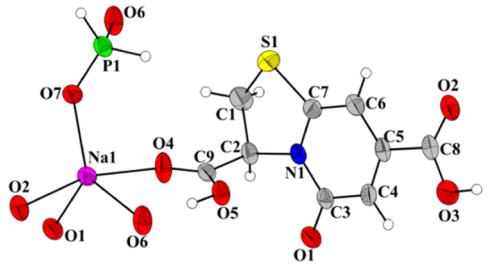

Figure 5. View of the molecular structure of (**3**), showing 70% probability displacement ellipsoids. H atoms are shown as small spheres of arbitrary radii.

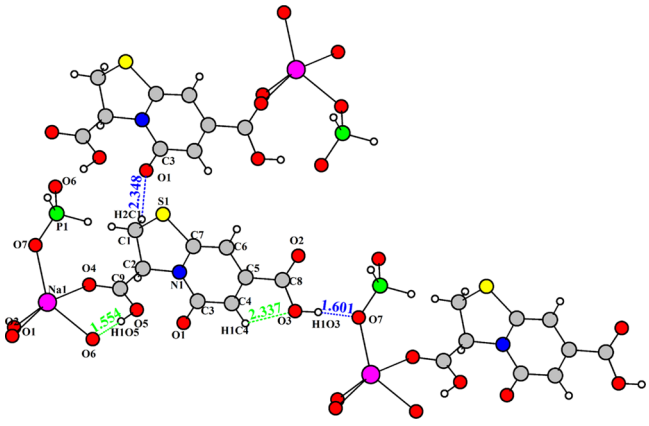

Figure 7. View of the hydrogen bonds in (**3**). The blue and green dashed lines correspond to inter- and intramolecular interactions, respectively.

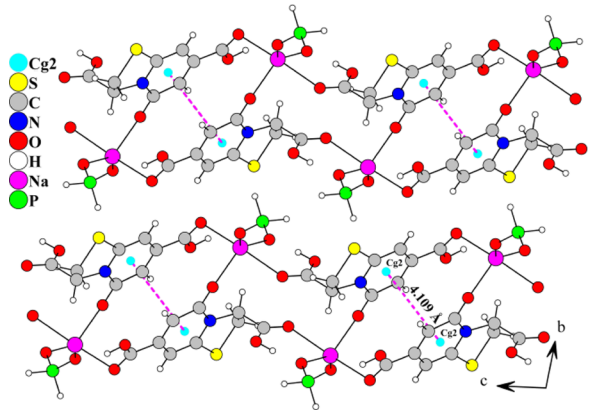

Figure 6. View of the layered structure of (**3**) along the *a* axis. The pink dashed lines correspond to $\pi-\pi$ interactions between the six-membered rings. *Cg*2 is the centroid of the six-membered ring.

to the (010) plane (Figure 6). Within a single layer, the TPDCA molecules are linked through sodium bridges in addition to the existence of offset $\pi-\pi$ interactions (see pink dashed lines in Figure 6). Each molecule of (**3**) is linked to two other molecules through one weak C−H···O═C and one moderate COO−H···O−Na hydrogen bonds (see blue dashed lines in Figure 7). Two additional intramolecular hydrogen bonds were also observed (see green dashed lines in Figure 7). Selected bond lengths and angles are given in Table 4.

The check cif indicated few Alerts Type A, which are related to short hydrogen bonds involving COOH. These short distances are commonly found in compounds containing carboxylic acid groups. It is worth to mention that no hydrogen bonds connecting the different layers were observed. Even the $\pi-\pi$ interactions [*Cg*2-*Cg*2*i* = 4.1091 (8) Å, interplanar distance = 3.120 (1) Å, slippage = 2.674 (1) Å, $\alpha = 0°$, *Cg*2 is the centroid of the six-membered ring (N1C3-C7), symmetry code (i): $1-x,1-y,1-z$ (Figure 6)] exist only within a single layer and not between the layers, which confirms that the structure is bi-dimensional.

2.2.4. Crystal Structure of Compound (4). Compound (**4**) crystallizes in the triclinic space group $P\bar{1}$ with two ammonium cations, one TPDCA, and one water molecule in the asymmetric unit (Figure 8). Selected hydrogen bond lengths and angles are given in Table 5. $N2H_4$ interacts with four different TPDCA molecules (see blue dashed lines in Figure 9a), whereas $N3H_4$ interacts with three TPDCA molecules through moderate N−H···O hydrogen bonds (see green dashed lines in Figure 9b). The water molecule also interacts with two different TPDCA molecules through moderate O−H···O hydrogen bonds (see red dashed lines in Figure 9b). These two types of hydrogen bonds allow the formation of layers parallel to the (001) plane. The $\pi-\pi$ interactions between the layers are too weak to be taken in consideration, and the structure is bi-dimensional [*Cg*2-*Cg*2i = 4.9487 (10) Å, interplanar distance = 3.351 (1) Å, slippage = 3.642 (1) Å, $\alpha = 0°$, *Cg* is the centroid of the six-membered ring (N1C3-C7), symmetry code (i): $1-x,1-y,2-z$] (see pink dashed lines in Figure 9c).

*2.2.5. Comparison of TPDCA Ligands in $C_9H_7NO_5S$, (**1**), (**2**), (**3**), and (**4**).* The structures of the TPDCA Ligands in the four compounds are very similar (see details in Table 6 and Figure S2). The five-membered rings have a substantially flattened envelope conformation with dihedral angles between the C2C1S1 fragments and the C2N1C7S1 planes varying from 21.38 to 37.33°. The interatomic S1-C1 and S1-C7 distances that vary from 1.810 (3) Å to 1.821 (2) Å and from 1.734 (2) Å to 1.750 (2) are typical of the S-Csp^3 and S-Csp^2 bonds, respectively.[11,22,23,26] The bond configurations at the N1 atoms are planar trigonal with the sum of the N1 bond angles almost 360°. The bicyclic S1N1C2-C8 systems can be regarded as planar since the dihedral angles between the six- and five-membered rings are less than 11°. The carboxyl groups C8O2O3 are slightly twisted from the bicyclic fragment with dihedral angles between 4.45 and 21.54°. The carboxyl

https://dx.doi.org/10.1021/acsomega.0c01769
ACS Omega 2020, 5, 27756−27765

Table 4. List of Detected Hydrogen Bonds in (3)

donor	hydrogen	acceptor	D−H distance	H···A distance	D−A distance	D−H···A angle
O3	H1O3	O7	0.960(18)	1.602(17)	2.5396(18)	164.3(16)
O5	H1O5	O6	0.960(13)	1.554(12)	2.5109(16)	174.1(18)
C1	H2C1	O1	0.96	2.35	3.221(2)	150.84
C4	H1C4	O3	0.96	2.34	2.688(2)	100.80

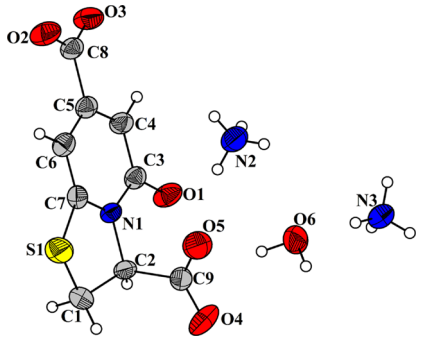

Figure 8. Molecular structure of (4) showing 70% probability displacement ellipsoids. H atoms are shown as small spheres of arbitrary radii.

groups C9O4O5H are almost perpendicular to the bicyclic fragments with dihedral angles between 74.58 and 86.74°.

2.3. Antibacterial Activity. Many compounds containing a ring-fused 2-pyridone fragment exhibit biological activity against the pili assembly machinery termed the chaperone usher[2] in uropathogenic *E. coli*. The antibacterial properties of the new TPDCA derivatives were evaluated against two types of bacteria (Gram-positive *S. aureus* and Gram-negative *E. coli*) using the agar well diffusion method. When tested against *E. coli,* compounds (**1**) and (**3**), at 5 mg each, showed about 12 and 8 mm inhibition zones, respectively (Figure 10a,b), while at 20 mg, the inhibition zones of (**1**) and (**3**) increased to 23 and 17 mm, respectively (Figure 10c,d). At the same concentration (20 mg), (**1**) and (**3**) showed about 15 and 10 mm inhibition zones against *S. aureus* (Figure 10e,f). In summary, (**1**) and (**3**) displayed stronger antibacterial activity against Gram-negative *E. coli* than against Gram-positive *S. aureus.*

2.4. Anticancer Activity. The motif of 2-pyridone is present in camptothecin, a natural compound isolated from the bark and stem of the *Camptotheca acuminata* tree, used as a cancer treatment in traditional Chinese medicine.[27] However, it has low solubility, so numerous analogues have been developed and two of them, topotecan and irinotecan, have been approved and are used in cancer chemotherapy today.[28] Unfortunately, cancer cells often develop resistance to chemotherapeutics and new synthetic compounds are being tested for their possible anticancer properties in order to find novel lead structures. In the present study, the cytotoxic activity of compounds (**1**−**3**) was evaluated in leukemia HL-60 cell line, using MTT assay. As shown in Figure 11, only compound (**1**) "$2(C_9H_7NO_5S)\cdot H_2O$" decreased the metabolic activity of HL-60 cells by 50% at 158.5 ± 12.5 μM concentration. This structure can be further modified in order to obtain more cytotoxic analogues.

3. CONCLUSIONS

Four new TPDCA derivatives: $2(C_9H_7NO_5S)H_2O$ (**1**), $(C_9H_7NO_5S)C_5H_9NO$ (**2**), $(C_9H_7NO_5S)Na(PO_2H_2)$ (**3**) and $(C_9H_5NO_5S)(NH_4)_2(H_2O)$ (**4**) were synthesized, and their crystal structures were determined. Different types of hydrogen bonds were observed in these compounds, which led to a three-dimensional network in (**1**), an infinite chain along [001] in (**2**), an infinite two dimensional network in the (010) plane in (**3**), and an infinite two dimensional network in the (001) plane in (**4**). Furthermore, very weak $\pi-\pi$ interactions between the six-membered rings were observed in compound (**3**) and C═O···π interactions were observed in (**1**) and (**2**). The antimicrobial test showed significant activity of derivatives (**1**) and (**3**) against *E. coli* and *S. aureus*. These compounds can be helpful in removing infectious bacteria from the wastewater thus can be widely utilized for wastewater treatments. Out of three tested compounds, only (**1**) showed some cytotoxicity against leukemia HL-60 cells.

4. EXPERIMENTAL SECTION

4.1. Synthetic Procedures. *4.1.1. Synthesis of 2-$(C_9H_7NO_5S)H_2O$ (1).* The un-solvated TPDCA ligand used for the synthesis was obtained following the procedure reported,[11] whereas the crystals of the solvated TPDCA molecule were obtained during the preparation of the TPDCA-$Co(HPO_3)_2$ compound. TPDCA (0.12 g), H_3PO_3 (0.082 g), and $Co(CH_3COO)_2\cdot 4H_2O$ (0.1245 g) were mixed together in 10 mL of distilled water. The mixture was then stirred for 1 h and left under the fume hood at room temperature. After 1

Table 5. List of Detected Hydrogen Bonds in (4)

donor	hydrogen	acceptor	D−H distance	H···A distance	D−A distance	D−H···A angle
N3	H1N3	O4	0.870(11)	1.946(10)	2.803(3)	168.1(8)
N3	H2N3	O6	0.87	1.91	2.781(2)	174.69
N3	H3N3	O2	0.87	2.02	2.8860(19)	170.84
N3	H4N3	O3	0.87	2.17	3.039(2)	174.06
N2	H1N2	O3	0.870(10)	2.210(10)	2.976(2)	146.7(7)
N2	H2N2	O1	0.87	2.01	2.8612(18)	167.36
N2	H3N2	O5	0.87	1.98	2.833(2)	165.90
N2	H4N2	O1	0.87	1.98	2.828(2)	163.39
O6	H1O6	O3	0.953(6)	1.790(7)	2.7261(19)	166.7(18)
O6	H2O6	O5	0.953(15)	1.778(17)	2.680(2)	156.8(14)

https://dx.doi.org/10.1021/acsomega.0c01769
ACS Omega 2020, 5, 27756−27765

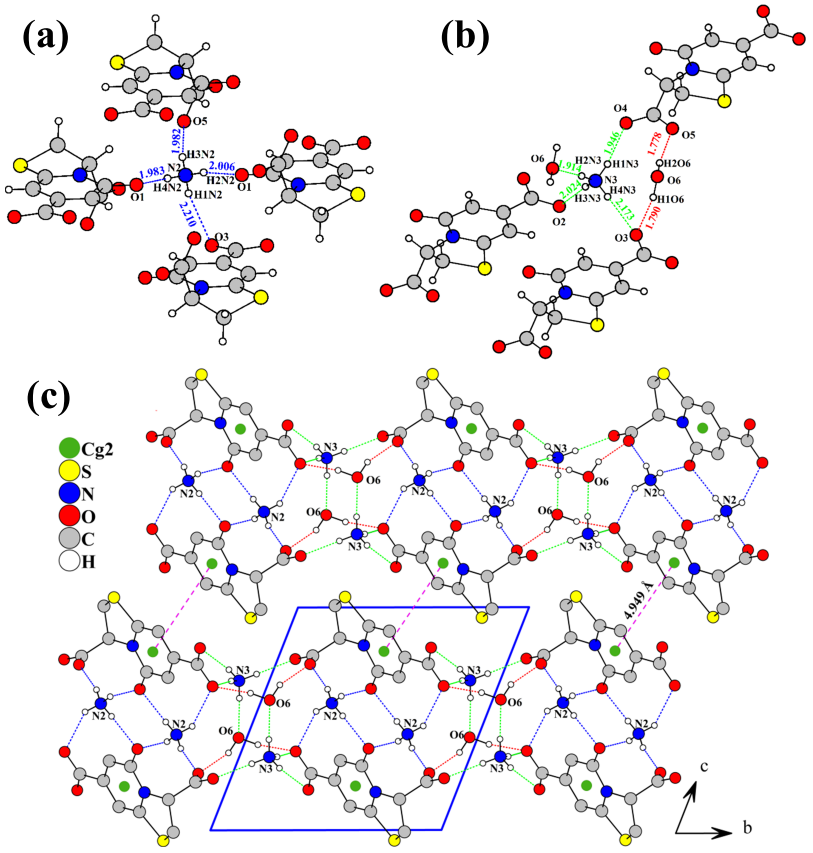

Figure 9. View of the hydrogen bonds in (**4**). (a, b) Blue, green, and red dashed lines correspond to the interactions involving $N2H_4$, $N3H_4$, and H_2O, respectively. (c) View along the *a* axis of the layers parallel to (001) plane. The pink dashed lines correspond to the distance *Cg*2-*Cg*2i between the six-membered rings of successive layers.

Table 6. Comparison of the Crystallographic Data of $C_9H_7NO_5S$, (1), (2), (3), and (4)

compounds	$C_9H_7NO_5S$ ligand1	(**2**) ligand1	(**3**) ligand1	(**4**) ligand1	(**1**) ligand1	(**1**) ligand2
dihedral angle between C2C1S1 and C2N1C7S1 planes (°)	37.33(1)	36.86(3)	34.76(1)	31.28	21.38(2)	31.59(1)
puckering parameters *Q* (Å) & φ(°) of the 5-membered ring of TPDCA	0.3950(14) & 217.9(2)	0.3870(16) & 214.8(2)	0.3681(14)& 216.8(2)	0.3304(16) & 214.9(3)	0.226(2) & 43.2(5)	0.3323(18) & 216.9(3)
pseudorotation parameters P (°) & Tau(M) (°)of the 5-membered ring of TPDCA	26.6(1) &37.4(1)	23.0(2) & 36.4(1)	25.6(1) & 34.8(1)	23.0(2) & 31.0(1)	212.6(3) & 22.2(1)	25.7(2) & 31.6(1)
conformation of the 5-membered ring of TPDCA	envelope on C1	envelope on C1	envelope on C1	envelope on C1	envelope on C1	envelope on C10
distance S1-C1 (Å)	1.818(2)	1.820(2)	1.821(2)	1.814(2)	1.810(3)	S2-C10 1.812(3)
distance S1-C7 (Å)	1.746(2)	1.742(2)	1.750(2)	1.7391(14)	1.734(2)	S2-C16 1.743(2)
sum of the N1 bond angles in (°)	359.45(1)	359.97(2)	359.86(1)	359.56(15)	359.73(3)	359.83(3)
dihedral angle between the six- and five-membered rings (°)	5.82(1)	10.10(2)	5.67(1)	5.10(3)	4.01(2)	6.02(1)
dihedral angle between the carboxyl group C8O2O3 and the bicyclic fragment (°)	10.32(2)	4.45(1)	12.5(3)	8.65(1)	6.01(1)	21.54(3)
dihedral angle between the carboxyl group C9O4O5 and the bicyclic fragment (°)	82.99(1)	79.73(1)	78.592)	86.74(3)	74.58(2)	80.68(1)
references	11	this work	this work	this work	this work	this work

week, several yellow crystals were formed. The solution was then filtered and the crystals were washed with acetone. The single-crystal XRD analyses performed on seven different crystals indicated that all of them correspond to (**1**). This batch was used for biological tests. The filtered solution was also evaporated for one more week. This led to a mixture of naked eye distinguishable large yellow and orange needles of (**1**) (~80%) and TPDCA (~20%), respectively.

*4.1.2. Synthesis of ($C_9H_7NO_5S$)C_5H_9NO (**2**).* This compound was prepared using wet chemistry from stoichiometric mixtures of TPDCA (0.12 g) and sodium hypophosphite $NaH_2PO_2.H_2O$ (0.088 g, Aldrich, 99.99%). TPDCA was dissolved in 5 mL of *N*-Methyl-2-pyrrolidone (NMP) to

https://dx.doi.org/10.1021/acsomega.0c01769
ACS Omega 2020, 5, 27756−27765

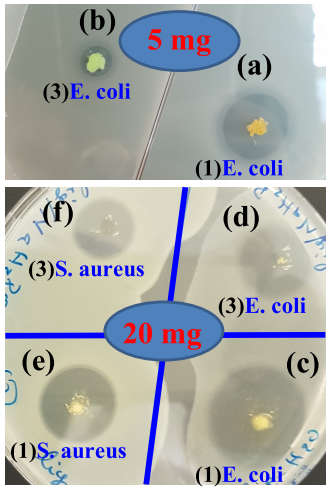

Figure 10. Inhibition zones of 5 mg of compounds (a) (**1**) and (b) (**3**) against *E. coli*, of 20 mg of compounds (c) (**1**) and (d) (**3**) against *E. coli*, and of 20 mg of compounds (e) (**1**) and (f) (**3**) against *S. aureus*, respectively.

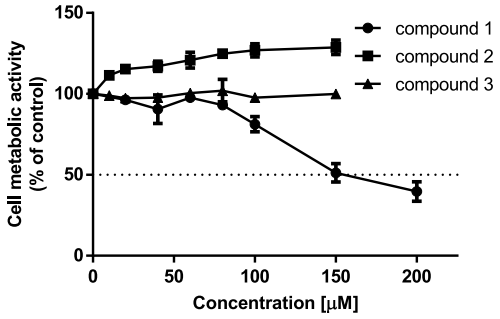

Figure 11. Comparison of the metabolic activity of HL-60 cells treated for 48 h with TPDCA analogues as determined by the MTT assay.

form the clear solution A, which was stirred at 50°C for 30 min. NaH_2PO_2. H_2O was dissolved in 10 mL of H_2O forming the solution B. Then, solution B was added to solution A dropwise and left stirring at 50 °C for one additional hour. The resulting clear solution was left still at room temperature. After 1 week, few tiny yellow crystals were formed. The solution was then filtered, and the crystals were washed with acetone. The single-crystal XRD analyses performed on several crystals indicated that all of them correspond to (**2**). This batch was used for biological tests. The filtered solution was also evaporated for one more week. This led to a mixture of large yellow and orange needles of (**2**) (~90%) and TPDCA (~10%), respectively.

*4.1.3. Synthesis of $(C_9H_7NO_5S)Na(PO_2H_2)$ (**3**).* This compound was prepared exactly following the procedure above. Only NMP was replaced by dimethylformamide (DMF). After 1 week, several large yellow crystals were formed. The solution was then filtered, and the crystals were washed with acetone. The single-crystal XRD analyses performed on several crystals indicated that all of them correspond to (**3**). This batch was used for biological tests. The filtered solution was also evaporated for one more week. This led to a mixture of large yellow and orange needles of (**3**) (~80%) and TPDCA (~20%), respectively.

*4.1.4. Synthesis of $(C_9H_5NO_5S)(NH_4)_2(H_2O)$ (**4**).* TPDCA (0.10 g) was dissolved in 0.2 mL of distilled water and 0.450 mL ammonia solution at 50 °C in a glass tube. Then, the water content was slowly evaporated to leave block crystals of (**4**) (72%) at the bottom of the tube.

4.2. Single-Crystal X-Ray Diffraction Measurements. Suitable (**1**), (**2**), (**3**), and (**4**) single crystals for X-ray diffraction were selected on the basis of the size and the sharpness of the diffraction spots. The data collections were carried out on a D8 Venture diffractometer using Mo Kα radiation. Data processing and all refinements were performed with the APEX3 and Jana2006 program package, respectively.[17,18] For (**1**) and (**2**), Gaussian-type absorption corrections were applied and the shape was determined with the video microscope; however, for (**3**) and (**4**), multiscan absorption corrections using SADABS were applied.[18] For data collection details, see Table 1.

4.3. Microorganisms and Inoculum Preparation. The antimicrobial properties of compounds (**1**) and (**3**) were evaluated using two types of bacteria (Gram-positive and Gram-negative). The bacterial strains used in the present study were isolated from the treated sewage effluent of Qatar foundation treatment plant and identified by using the 16S RNA ribosomal method (unpublished data). For inoculum preparation, a single bacterial colony was picked from nutrient agar using disposable sterile loop, transferred into 10 mL of nutrient broth and placed overnight in incubator shaker at 37 °C with a shaking speed of 100 rpm. The bacterial cell density was measured at an optical density (OD) of 600 nm using a spectrophotometer. Each inoculum prepared would contain approximately 107 cfu/mL of bacteria. Bacterial sensitivity to compounds (**1**) and (**3**) is performed by employing the agar well diffusion method. Three millimeter-diameter holes were made in the agar plates using 50 mL disposable pipette, and different amounts varying from 5 to 20 mg of this material were placed carefully in the holes. Ampicillin (10 μg/mL) was used as a standard antibiotic. The plates were overlaid with a mixture of each bacteria with 2 mL of molten 1.5% (wt/vol) noble agar (Sigma-Aldrich) at proximately 37 °C. Finally, the plates were incubated at 37 °C for 24 h and the average diameter of the inhibition zone surrounding the holes was examined.

4.4. Cell Culture and Cell Metabolic Activity – MTT Assay. Caucasian promyelocytic leukemia (HL-60) was obtained from the European Collection of Cell Cultures (ECACC). Cells were maintained in an RPMI 1640 + Glutamax medium (Gibco/Life Technologies, Carlsbad, CA, USA), supplemented with 10% fetal bovine serum (FBS), streptomycin, and penicillin at 37 °C in a 5% CO_2-humidified atmosphere. The influence of the compounds on cell metabolic activity was investigated using the MTT (3-(4,5-dimethyldiazol-2-yl)-2,5 diphenyl tetrazolium bromide) assay. In brief, HL-60, cells were seeded in 24-well plates (TPP Techno Plastic Products AG, Switzerland) at a concentration of 8×10^4/ml and incubated for 20 h at 37 °C. The cells were treated with a range of concentrations of the compounds. Compound (**1**) was dissolved in DMSO, while compounds (**2**) and (**3**) were dissolved in water. Cells treated with a vehicle were used as a control. Then, the cells were incubated for an additional 48 h at 37 °C. MTT solution (100 μL; 5 mg/1 mL in PBS) was added to each well, followed by 1 h of incubation. The plates were centrifuged (3000 rpm, 5 min), and the supernatant was discarded. DMSO (1 mL) was added to each well to dissolve the formazan product. The absorbance was measured at 560 nm using a FlexStation 3 Multi-Mode

https://dx.doi.org/10.1021/acsomega.0c01769
ACS Omega 2020, 5, 27756−27765

Microplate Reader (Molecular Devices, LLC). Assays were performed twice in triplicate for each dose. Data analysis was performed using Prism 5.0 (GraphPad Software Inc., San Diego, CA, USA). Results from two independent experiments in triplicate were expressed as mean ± SEM.

■ ASSOCIATED CONTENT

Supporting Information

The Supporting Information is available free of charge at https://pubs.acs.org/doi/10.1021/acsomega.0c01769.

Atomic positions and anisotropic displacement parameters (Tables S1-S8), interactions between TPDCA and NMP in compound (**2**) (Figure S1), comparison of TPDCA ligands in $C_9H_7NO_5S$, (**1**), (**2**), (**3**), and (**4**) (Figure S2), and synthesis and characterization processes for compounds 1−3 (Figure S3) (PDF)

Crystallographic data of compound (**1**) (CIF)

Crystallographic data of compound (**2**) (CIF)

Crystallographic data of compound (**3**) (CIF)

Crystallographic data of compound (**4**) (CIF)

■ AUTHOR INFORMATION

Corresponding Author

Hamdi Ben Yahia − *Qatar Environment and Energy Research Institute (QEERI 2.0), Hamad Bin Khalifa University, 34110 Doha, Qatar;* orcid.org/0000-0001-6577-9498; Email: hyahia@hbku.edu.qa, hyahia@qf.org.qa

Authors

Souhir Sabri − *Qatar Environment and Energy Research Institute (QEERI 2.0), Hamad Bin Khalifa University, 34110 Doha, Qatar*

Rachid Essehli − *Energy and Transportation Science Division, Oak Ridge National Laboratory, Oak Ridge 37831-2008, Tennessee, United States*

Peter Kasak − *Centre for Advanced Materials (CAM), Qatar University, 2713 Doha, Qatar;* orcid.org/0000-0003-4557-1408

Joanna Drogosz-Stachowicz − *Department of Biomolecular Chemistry, Medical University of Lodz, 92-215 Lodz, Poland*

Anna Janecka − *Department of Biomolecular Chemistry, Medical University of Lodz, 92-215 Lodz, Poland*

Brahim El Bali − *Independent scientist, Oujda 60000, Morocco;* orcid.org/0000-0001-6926-6286

Complete contact information is available at: https://pubs.acs.org/10.1021/acsomega.0c01769

Author Contributions

The manuscript was written through contributions of all authors. All authors have given approval to the final version of the manuscript.

Funding

The publication of this article was funded by the Qatar National Library. This work was also made possible by NPRP grant no. 8-878-1-172 from the Qatar National Research Fund (A Member of The Qatar Foundation). The finding achieved herein is solely the responsibility of the authors. The biological investigations were supported by a grant from the Medical University of Lodz No. 503/1-156-02/503-11-002.

Notes

The authors declare no competing financial interest.

■ ACKNOWLEDGMENTS

The authors would like to thank Dr. Said Mansour for the access to the characterization tools in the core lab. R.E. would like to thank the Oak Ridge National Laboratory managed by UT Battelle, LLC, for the U.S. Department of Energy (DOE) under contract DE-AC05-00OR22725. The publication of this article was funded by the Qatar National Library.

■ ABBREVIATIONS

TPDCA, 5-oxo-2,3-dihydro-5H-[1,3]-thiazolo[3,2-a]pyridine-3,7-dicarboxylic acid; (**1**), [rac-(3R)-3-(dihydroxymethyl)-5-hydroxy-3,5,6,7,8,8a-hexahydro-2H-thiazolo[3,2-a]pyridin-7-yl]methanediol;[rac-(3S)-3-(dihydroxymethyl)-5-hydroxy-3,5,6,7,8,8a-hexahydro-2H-thiazolo[3,2-a]pyridin-7-yl]-methanediol;hydrate: $2(C_9H_7NO_5S)H_2O$; (**2**), 1-methylpyrrolidin-2-ol;[rac-(3S)-5-hydroxy-7-(3-hydroxydioxiran-3-yl)-3,5,6,7,8,8a-hexahydro-2H-thiazolo[3,2-a]pyridin-3-yl]-methanediol: $(C_9H_7NO_5S)C_5H_9NO$; (**3**), trihydroxy-[[rac-(3S)-3,7-bis[hydroxyl(sodiooxy)methyl]-3,5,6,7,8,8a-hexahydro-2H-thiazolo[3,2-a]pyridin-5-yl]oxy]-(sodiooxy-lambda5-phosphanyl)oxy-sodium: $(C_9H_7NO_5S)Na(PO_2H_2)$; (**4**), lambda5-azane;[rac-(3S)-3-(dihydroxymethyl)-5-hydroxy-3,5,6,7,8,8a-hexahydro-2H-thiazolo[3,2-a]pyridin-7-yl]-methanediol;hydrate: $(C_9H_5NO_5S)(NH_4)_2(H_2O)$; NMP, *N*-methyl-2-pyrrolidone; ADPs, atomic displacement parameters

■ REFERENCES

(1) Sirikantaramas, S.; Asano, T.; Sudo, H.; Yamazaki, M.; Saito, K. Camptothecin: therapeutic potential and biotechnology. *Curr. Pharm. Biotech.* **2007**, *8*, 196−202.

(2) Hedenström, M.; Emtenas, H.; Pemberton, N.; Aberg, V.; Hultgren, S. J.; Pinkner, J. S.; Tegman, V.; Almqvist, F.; Sethson, I.; Kihlberg, J. NMR studies of interactions between periplasmic chaperones from uropathogenic E. coli and pilicides that interfere with chaperone function and pilus assembly. *Org. Biomol. Chem.* **2005**, *3*, 4193−4200.

(3) Pinkner, J. S.; Remaut, H.; Buelens, F.; Miller, E.; Åberg, V.; Pemberton, N.; Hedenström, M.; Larsson, A.; Seed, P.; Waksman, G.; Hultgren, S. J.; Almqvist, F. Rationally designed small compounds inhibit pilus biogenesis in uropathogenic bacteria. *Proc. Natl. Acad. Sci. U. S. A.* **2006**, *103*, 17897−17902.

(4) Hola, K.; Zhang, Y.; Wang, Y.; Giannelis, E. P.; Zboril, R.; Rogach, A. L. Carbon dots—Emerging light emitters for bioimaging, cancer therapy and optoelectronics. *Nano Today* **2014**, *9*, 590−603.

(5) Reckmeier, C. J.; Schneider, J.; Susha, A. S.; Rogach, A. L. Luminescent colloidal carbon dots: optical properties and effects of doping [Invited]. *L. Opt. Express.* **2016**, *24*, A312−A340.

(6) Kasprzyk, W.; Bednarz, S.; Zmudzki, P.; Galica, M.; Bogdał, D. Novel efficient fluorophores synthesized from citric acid. *RSC Adv.* **2015**, *5*, 34795−34799.

(7) Schneider, J.; Reckmeier, C.; Xiong, Y.; von Seckendorff, M.; Susha, A.; Kasak, P.; Rogach, A. L. Molecular Fluorescence in Citric Acid-Based Carbon Dots. *J. Phys. Chem. C* **2017**, *121*, 2014−2022.

(8) Wang, H.-X.; Yang, Z.; Liu, Z.-G.; Wan, J.-Y.; Xiao, J.; Zhang, H.-L. Facile Preparation of Bright-Fluorescent Soft Materials from Small Organic Molecules. *Chem. − Eur. J.* **2016**, *22*, 8096−8104.

(9) Yang, J.; Zhang, Y.; Gautam, S.; Liu, L.; Dey, J.; Chen, W.; Mason, R. P.; Serrano, C. A.; Schug, K. A.; Tang, L. Development of aliphatic biodegradable photoluminescent polymers. *Proc. Natl. Acad. Sci. U. S. A.* **2009**, *106*, 10086−10091.

(10) Kasprzyk, W.; Bednarz, S.; Bogdał, D. Luminescence phenomena of biodegradable photoluminescent poly(diol citrates). *Chem. Commun.* **2013**, *49*, 6445−6447.

(11) Shi, L.; Yang, J. H.; Zeng, H. B.; Chen, Y. M.; Yang, S. C.; Wu, C.; Zeng, H.; Yoshihito, O.; Zhang, Q. Carbon dots with high

fluorescence quantum yield: the fluorescence originates from organic fluorophores. *Nanoscale* **2016**, *8*, 14374−14378.
(12) Kim, J. P.; Xie, Z.; Creer, M.; Liu, Z.; Yang, J. Citrate-based fluorescent materials for low-cost chloride sensing in the diagnosis of Cystic Fibrosis. *Chem. Sci.* **2017**, *8*, 550−558.
(13) Piatek, R.; Zalewska-Piatek, B.; Dzierzbicka, K.; Makowiec, S.; Pilipczuk, J.; Szemiako, K.; Cyranka-Czaja, A.; Wojciechowski, M. Pilicides inhibit the FGL chaperone/usher assisted biogenesis of the Dr fimbrial polyadhesin from uropathogenic *Escherichia coli*. *BMC Microbiology* **2013**, *13*, 131.
(14) Guzik, K.; Tomala, M.; Muszak, D.; Konieczny, M.; Hec, A.; Błaszkiewicz, U.; Pustuła, M.; Butera, R.; Dömling, A.; Holak, T. A. Development of the Inhibitors That Target the PD-1/PD-L1 Interaction—A Brief Look at Progress on Small Molecules, Peptides and Macrocycles. *Peptides and Macrocycles* **2019**, *24*, 2071.
(15) Horvat, I.; Sellstedt, M.; Weise, C.; Nordvall, L.-M.; Prasad, G. K.; Olofsson, A.; Larsson, G.; Almqvist, F.; Wittung-Stafshede, P. Modulation of α-Synuclein Fibrillization by Ring-Fused 2-pyridones: Templation and Inhibition Involve Oligomers With Different Structure. *Arch. Biochem. Biophys.* **2013**, *532*, 84−90.
(16) Kulén, M.; Núñez-Otero, C.; Cairns, A. G.; Silver, J.; Lindgren, A. E. G.; Wede, E.; Singh, P.; Vielfort, K.; Bahnan, W.; Good, J. A. D.; Svensson, R.; Bergström, S.; Gylfe, Å.; Almqvist, F. Methyl sulfonamide substituents improve the pharmacokinetic properties of bicyclic 2-pyridone based *Chlamydia trachomatis* inhibitors. *Med. Chem. Commun.* **2019**, *10*, 1966−1987.
(17) Bruker, *APEX2, SAINT-Plus, XPREP and SADABS*, Bruker AXS Inc., Madison, Wisconsin, USA, (2004).
(18) Petříček, V.; Dušek, M.; Palatinus, L. Crystallographic Computing System JANA2006: General features. *Z. Kristallogr. - Cryst. Mater.* **2014**, *229*, 345−352.
(19) Spek, A. L. *PLATON, A Multipurpose Crystallographic Tool*, Utrecht University, Utrecht, The Netherlands, (2008).
(20) Flack, H. D. On enantiomorph-polarity estimation. *Acta Cryst.* **1983**, *39*, 876−881.
(21) Brandenburg, K. *DIAMOND*. Version. 2.1c. Crystal Impact GbR, Bonn, Germany, 1999.
(22) Dotsenko, V. V.; Krivokolysko, S. G.; Chernega, A. N.; Litvinov, V. P. Anilinomethylidene derivatives of cyclic 1,3-dicarbonyl compounds in the synthesis of new sulfur-containing pyridines and quinolines. *Russian Chem. Bull, Int. Ed.* **2002**, *51*, 1556−1561.
(23) Åberg, V.; Boström, D.; Fischer, A.; Almqvist, F. Synthesis and absolute configuration of methyl (−)-(3*R*)-8-(4-bromophenyl)-7-(naphthalen-1-ylmethyl)-5-oxo-2,3-dihydro-5*H*-thiazolo(3,2-*a*)-pyridine-3-carboxylate. *Acta Cryst.* **2002**, *58*, o812−o814.
(24) Steiner, T. The hydrogen bond in the solid state. *Angew. Chem. Int. Ed.* **2002**, *41*, 48−76.
(25) Jeffrey, G. A. *An Introduction to Hydrogen Bonding*, Oxford University Press, Oxford, (1997).
(26) Seger, H.; Stempfhuber, S.; Zabel, M.; Marsch, M.; Geyer, A.; Harms, K. (3R)-Methyl 6-tert-butoxycarbonylamino-5-oxo-2,3-dihydro-5H-1,3-thiazolo(3,2-a)pyridine-3-carboxylate. *Acta Cryst.* **2005**, *61*, o2576−o2578.
(27) Ulukan, H.; Swaan, P. W. Camptothecins. *Drugs* **2002**, *62*, 2039.
(28) Wall, M. E.; Wani, M. C.; Cook, C. E.; Palmer, K. H.; McPhail, A. I.; Sim, G. A. Plant Antitumor Agents. I. The Isolation and Structure of Camptothecin, a Novel Alkaloidal Leukemia and Tumor Inhibitor from Camptotheca acuminate. *J. Am. Chem. Soc.* **1966**, *88*, 3888−3890.

https://dx.doi.org/10.1021/acsomega.0c01769
ACS Omega 2020, 5, 27756−27765